



## Experimental investigation of effect of specimen thickness on fracture toughness of Al-TiC composites

M. S. Raviraj

Department of Mechanical Engineering, Government Engineering College, Chamarajanagar 571313, India  
ravirajsunkapur@gmail.com

C. M. Sharanaprabhu

Department of Mechanical Engineering, Bapuji Institute of Engineering and Technology, Davangere 577004, India

G. C. Mohankumar

Department of Mechanical Engineering, National Institute of Technology Karnataka, Surathkal 575025, India

**ABSTRACT.** In this paper, the macro and micro-mechanical fracture behavior was studied for aluminum (Al6061) alloy matrix, reinforced with various proportions of TiC particles such as 3wt%, 5wt% and 7wt%. The Al6061-TiC metal matrix composites were produced by stir casting method to ensure uniform distribution of the TiC particulates in the Al matrix. The compact tension (CT) specimens were machined according to ASTM E399 specifications to evaluate the fracture toughness for Al6061-TiC metal matrix composites. The CT specimens were machined for crack to width ( $a/W$ ) ratio of 0.5 and thickness to width ( $B/W$ ) ratios of 0.2 to 0.7 with an increment of 0.1. Load versus crack mouth opening displacement (CMOD) data was plotted to estimate stress intensity factor  $K_Q$  for various thicknesses of the specimen. The fracture toughness  $K_{IC}$  was obtained by plotting stress intensity factor versus thickness to width ratios of specimen data. The fracture toughness of these composites varied between 16.4-19.2 MPa $\sqrt{m}$ . Scanning Electron Microscope (SEM) studies was made on the fractured surface of the specimens to understand the micro-mechanisms of failure involved in these composites. Void initiation is more significant in the matrix near the interface. The micro-cracks grow from these micro-voids and crack propagates by linking these micro cracks locating the crack path preferentially in the matrix adjacent to the interface indicating ductile fracture.

**KEYWORDS.** Fracture toughness; Titanium Carbide particulates; Aluminum matrix composites; Micro-mechanism.

### INTRODUCTION

Nowadays Aluminum alloy Metal Matrix Composites (MMCs) are replacing their monolithic counterparts for having enhanced mechanical properties and extended reliability combined with ease of processing. The incorporation of ceramic particles into the Al alloy matrix significantly alters the mechanical behavior of the materials. Addition of Titanium Carbide (TiC) particulates into the aluminum alloy results in grain refinement [1] and

there is sufficient lattice matching (coherency) for the direct nucleation of solid Al grains to occur on the particle surface [2,3] thus resulting in change in microstructure and properties of the composite. The Al-TiC MMCs occupy a unique position in the family of metal matrix composites as they find numerous applications in commercial aerospace, space technology, automobile, general industrial and engineering structures [4, 5]. Investigators [6, 7] showed the stir casting technique is the simplest and most commercial used technique to incorporate the ceramic particulate into liquid aluminum melt and allowing the mixture to solidify. Fatchurrohman [8] has justified that the solidification characteristics of TiC particulate reinforced Al alloy matrix composites are correlated with its hardness by stir casting technique. Some of the basic mechanical properties and micro-structural findings of Al6061 alloy matrix reinforced with various proportions of TiC particulates estimated by stir casting technique have been reported in our earlier publications [9]. However, evaluation of fracture toughness is essential for the reliable use of these composites for structural parts and components. Researchers [10-13] estimated fracture toughness for Al alloy matrix composites with SiC and  $\text{Al}_2\text{O}_3$  reinforcement particles. They showed that the reinforcement particles play significant effects in controlling the fracture toughness of the composites. To the best of our knowledge, not much of the work on fracture toughness values of Al-TiC composites are reported in open literature. In the present work an attempt is made to produce Al6061 alloy MMCs with different wt% TiC particles by stir casting method and the experimental work carried out to evaluate the fracture toughness and micro-structural features of fracture surfaces.

## EXPERIMENTAL WORK

The Al-TiC metal matrix composites were produced by stir casting method so as to achieve uniform distribution of TiC particulates in the Al matrix. Commercially available Al6061 alloy was melted in the graphite crucible and TiC particulates ( $2\mu\text{m}$  average in size) in the form of powder with three different wt% were added while stirring the melt at a speed of 750rpm. The melt at temperature of about  $920^\circ\text{C}$  was poured to rectangular shaped moulds of required size. Composites of various rectangular sheets or blocks with 3wt%, 5wt% and 7wt% of TiC were produced. The chemical composition and the mechanical properties of Al6061-TiC metal matrix composites are reported in our earlier work [9].

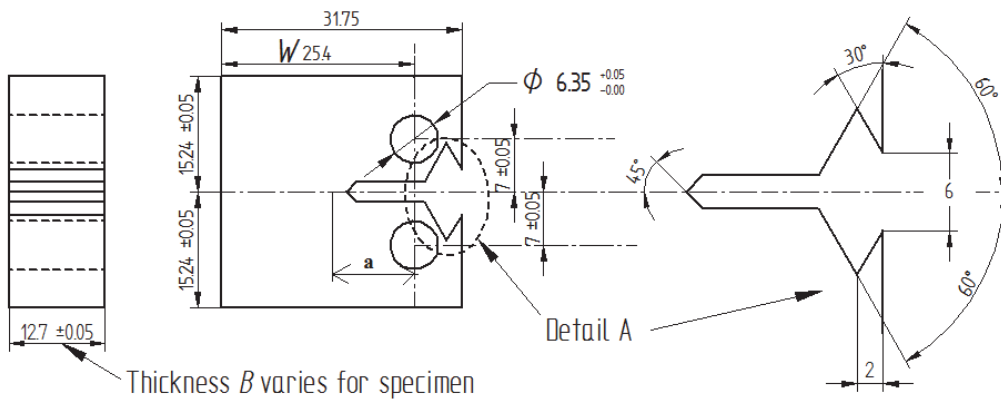


Figure 1: CT specimen specifications.

The compact tension specimens were machined out by CNC wire EDM from the rectangular blocks of various wt% TiC composites as per ASTM Standard E399 [14]. The detail dimensions and schematic views of the CT specimen are shown in Fig. 1. The CT specimens with variable thickness were machined so as to obtain different  $B/W$  of 0.2, 0.3, 0.4, 0.5, 0.6 and 0.7, as shown in Fig. 2(a). The straight through V-notch was machined so as to achieve  $a/W$  of 0.5 after fatigue pre-cracking for a length of 2.5mm, as seen in Fig. 2(b). The intended notch in the test specimen is to simulate an ideal crack with essentially zero root radius [15]. The fatigue pre-cracking of the CT specimens was done in a BiSS (Bangalore Integrated Systems Solutions) servo-hydraulic testing machine with tensile cyclic loading. The fatigue loads were maintained at 0.4 times the yield load of the material with the load ratio ( $R$ ) (min. tensile load/max. tensile load) of 0.1 maintaining the frequency of 10 Hz to obtain pre-crack length of 2.5mm successfully. The method of pre-cracking is similar to the earlier work [16]. Different load ranges were used depending on the specimen thickness. Once the crack



initiates and propagates by 2.5mm the fatigue loading would stop by the control options as given in the software to operate the testing machine.

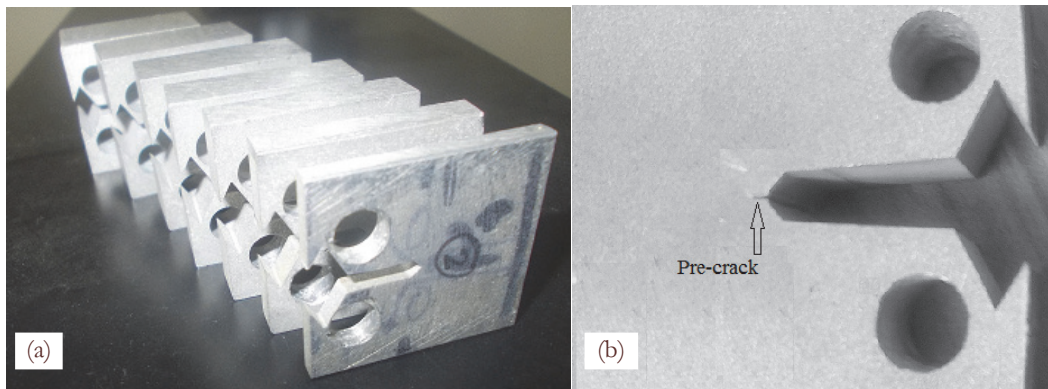


Figure 2: (a) Machined CT specimens of various thicknesses. (b) Fatigue pre-crack.

All fracture toughness tests were conducted using BiSS servo-hydraulic testing machine at room temperature. The machine capacity is of 100kN and is equipped with a load cell, Crack Mouth Opening Displacement (CMOD) gauge and a Linear Variable Differential Transformer (LVDT). All mentioned equipments associated with the test are calibrated. The CMOD gauge attached to a specimen was mounted in the loading system by the use of special grips as shown in Fig. 3.

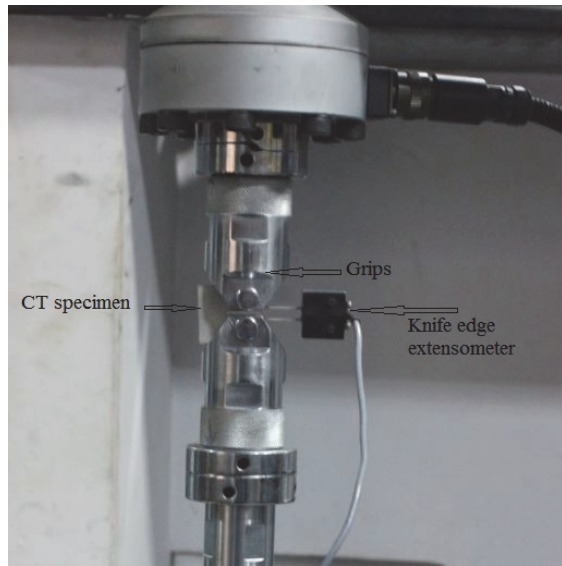


Figure 3: Test set up showing the mounted specimen in grips with COD gauge.

The fatigue pre-cracked CT specimens were tested under monotonically increasing tensile load using the commercial programme for determination of stress intensity factor. For the practical analyses, 5 identical CT specimens were considered for various Al6061-TiC composites and  $B/W$  ratios of  $a/W=0.5$ . Totally 90 specimens are considered for the practical analysis to estimate the fracture toughness of Al6061-TiC composite. All the test control was by stroke mode with a rate of 0.01667mm/sec. All the specimens were examined optically and by using Scanning Electron Microscope (SEM) to study the nature of the cracks and other details of bonding between matrix and particulates. The topography of fractured specimens and the microstructures were examined in detail using scanning electron microscope of ZEISS EVO18 make and an optical microscope (OM). This is done to characterize the fracture mechanisms of the composites. The particle and matrix interface details and the profile of crack propagation through the matrix and near the particles can

be assessed. Also by observing the fractographs the nature of fracture such as ductile and brittle fracture can be distinguished.

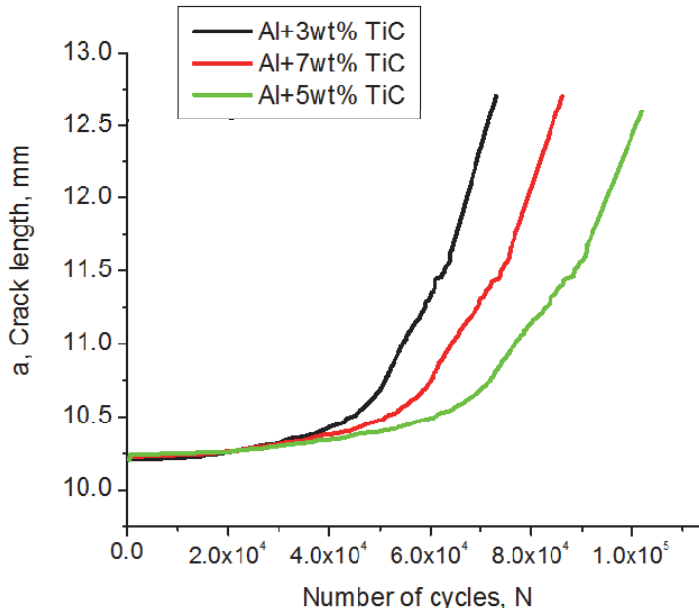


Figure 4: Crack length vs. Number of cycles for various Al6061-TiC composites typically for  $a/W = B/W=0.5$ .

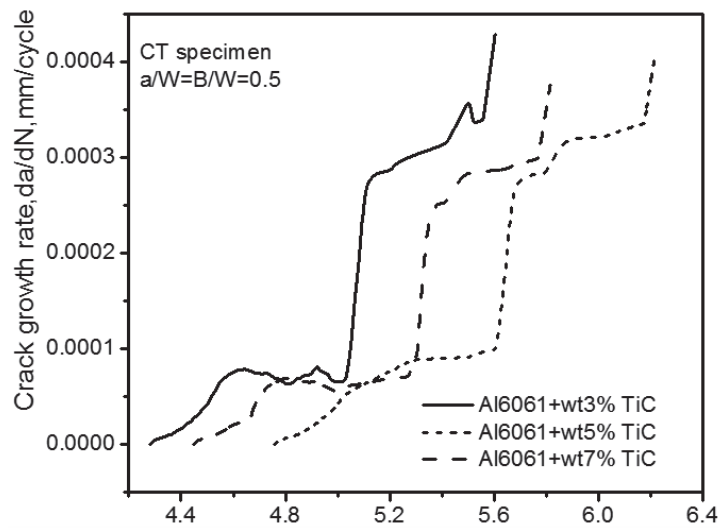


Figure 5:  $da/dN$  vs.  $\Delta K$  for various Al6061-TiC composites with typically for  $a/W = B/W=0.5$ .

## RESULTS AND DISCUSSION

The fatigue pre-crack should provide the occurrence of cracking at right place for all CT specimens of various Al6061-TiC composites and  $B/W$  ratios of  $a/W=0.5$ . During fatigue pre-cracking of the specimens, the increase in the crack length from 10.2mm to 12.7mm was measured with respect to the number of cycles for a load range ( $R$ ) of 0.1. Fig. 4 shows the variation of crack length versus number of cycles for CT specimens of  $a/W=B/W=0.5$  with various wt% TiC particles. It is clearly seen from Fig. 4 that number of cycles ( $N$ ) increased with weight percentage of TiC in the composites. The nature of variation of crack length versus number of cycles is similar to the earlier work of Mohanty *et.al.* [17], which was carried out for single edge notch specimen of Al7020-alloy. As the crack propagate in the



matrix, the reinforcing particles act as obstacles to reduce the local stress in the matrix and cause deviation of crack path as the crack deflects around the particles. This would increase the effect of roughness-induced closure and hence increase the threshold for crack propagation. Furthermore, the fatigue crack growth rates ( $da/dN$ ) were measured with stress intensity factor range ( $\Delta K$ ) for various CT specimens of Al6061-TiC composite. Fig. 5 shows the variation  $da/dN$  vs.  $\Delta K$  for CT specimens of  $a/W=B/W=0.5$  with various wt% TiC particles. From Fig. 5, it is clear that Al6061+5 wt% TiC shows higher  $\Delta K$  value compare to other two compositions of Al6061-TiC composites since Al6061+5 wt% TiC composite has higher Young's modulus as revealed in our earlier work, will increase  $\Delta K$  value. The results shown in Fig. 5 are similar to the earlier work of Harrison [16]. Subsequently, SEM micrograph shows clear distinction of the three regions *i.e.*, machined notch surface, fatigue pre-crack surface and fracture mode surfaces in Fig. 6 for CT specimen of Al6061+5 wt %TiC composite with  $a/W=B/W= 0.5$ . It is observed that that the fatigue crack growth results in curved crack front indicating the plane strain condition exists in the center where crack grows more and is subsequently arrested at the surface. The fatigue crack growth curve for various Al6061-TiC composites and  $B/W$  ratios of  $a/W=0.5$  fall over a narrower stress intensity range. Hence, the composite may therefore, be considered as potential candidate materials for aerospace sectors [13].

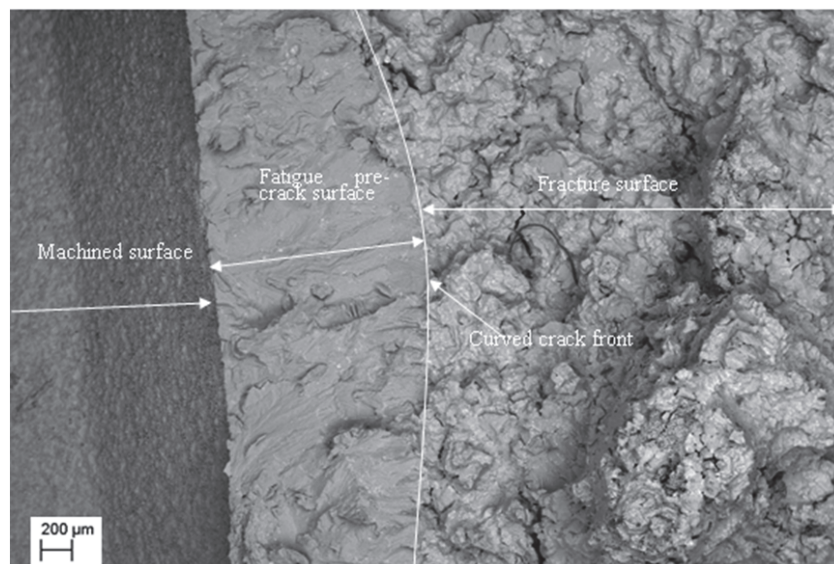


Figure 6: SEM micrograph of different surfaces for Al6061+wt5%TiC composite with  $a/W=B/W= 0.5$ .

Next, the CT specimens of various Al6061-TiC metal matrix composites and  $B/W$  ratios of  $a/W=0.5$  were subjected to loading to estimate the critical load ( $P_Q$ ) by plotting load *vs.* crack mouth opening displacement. The average value of five identical CT specimens of various Al6061-TiC composites and  $B/W$  ratios was considered to plot load *vs.* crack mouth opening displacement. Figs. 7-9 show the variation of load *vs.* crack mouth opening displacement for various Al6061-TiC composites and  $B/W$  ratios. It is observed from Fig. 7-9 that the maximum load increases with increase in  $B/W$  ratios. The specimens with  $B/W \leq 0.4$  undergo plane stress fracture due to high plasticity and less stress triaxiality compared to the specimens with  $B/W \geq 0.5$ . The  $P_Q$  value was obtained by drawing the 5% of the secant line to the maximum load on experimental data using curve fitting phenomena, which is not shown in figure. The magnitude of stress intensity factor  $K_Q$  for CT specimens of various Al6061-TiC composites and  $B/W$  ratios were calculated experimentally by substituting the  $F_Q$  value and dimensions of CT specimen in Eq. (1) [14].

$$K_Q = \frac{P_Q}{B\sqrt{W}} \times f\left(\frac{a}{W}\right) \quad (1)$$

The  $f\left(\frac{a}{W}\right)$  polynomial equation:

$$f\left(\frac{a}{W}\right) = \frac{2 + \left(\frac{a}{W}\right)}{\left[1 - \left(\frac{a}{W}\right)\right]^{3/2}} \left[ 0.886 + 4.64\left(\frac{a}{W}\right) - 13.32\left(\frac{a}{W}\right)^2 + 14.72\left(\frac{a}{W}\right)^3 - 5.60\left(\frac{a}{W}\right)^4 \right] \quad (2)$$

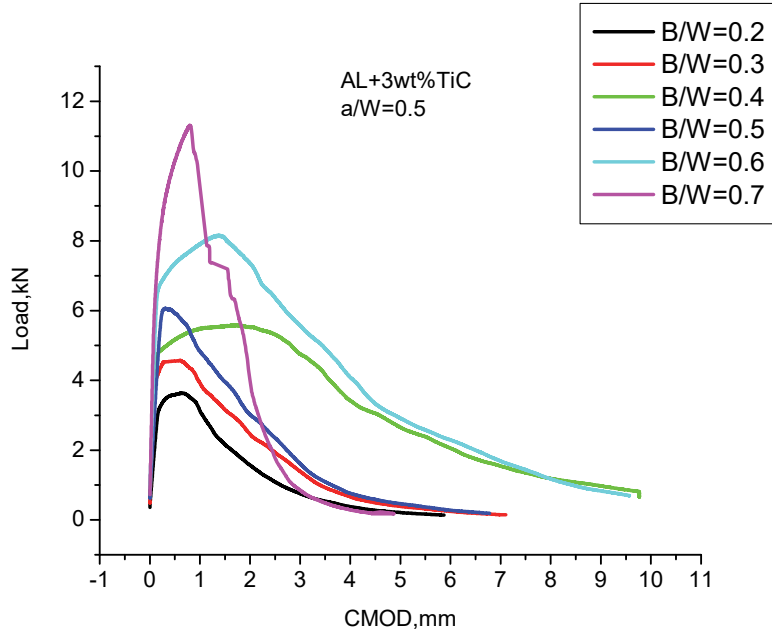


Figure 7: Load vs. crack mouth opening displacement curves for Al6061+wt3% TiC composite of various  $B/W$  ratios.

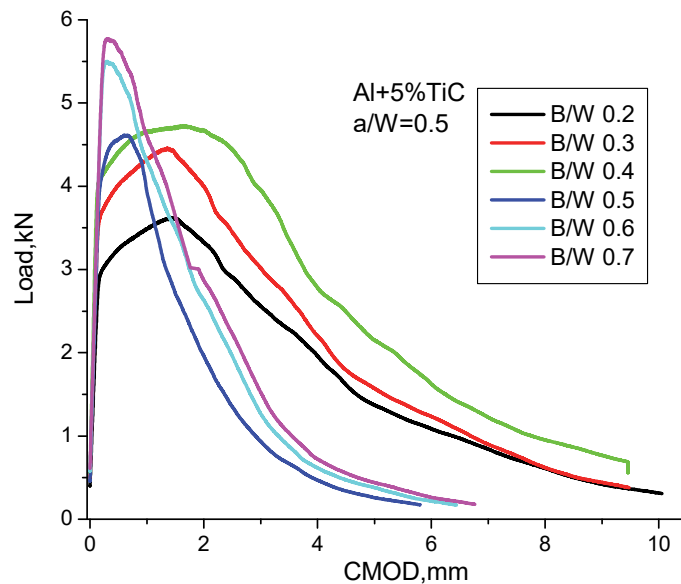


Figure 8: Load vs. crack mouth opening displacement curves for Al6061+wt5% TiC composite of various  $B/W$  ratios.

The calculated  $K_Q$  is plotted against various  $B/W$  ratios for various Al6061-TiC composites. Fig. 10 shows the variation of  $K_Q$  vs.  $B/W$  ratios for various Al6061-TiC composites. It is observed from Fig. 10 that the  $K_Q$  decreases with increase in  $B/W$  ratios and found to remain constant for  $B/W \geq 0.5$ . This constant value of  $K_Q$  for  $B/W \geq 0.5$  prevail the plane strain fracture toughness ( $K_{IC}$ ) of the composite. For  $B/W \leq 0.4$ , the value of  $K_{IC}$  can be considered the real plane stress fracture toughness. It is analyzed from Fig. 10 that the increase of TiC from 3wt% to 5wt% in Al6061 matrix composites, there will be a decrease in fracture toughness from 19.2 MPa $\sqrt{m}$  to 16.4 MPa $\sqrt{m}$  and further increase of TiC to 7wt% the



fracture toughness increases slightly to  $17.6 \text{ MPa}\sqrt{\text{m}}$ . Since, Al6061+wt5%TiC composites exhibits higher yield stress compare to other two compositions as discussed in our earlier work. The results show the variation of wt% TiC reinforcement particles with Al6061 matrix significantly affects the fracture toughness.

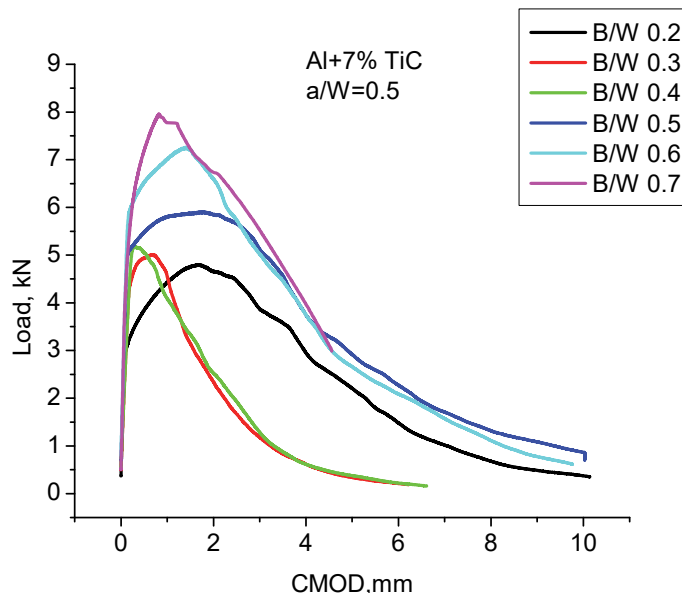


Figure 9: Load vs. crack mouth opening displacement curves for Al6061+wt7% TiC composite of various  $B/W$  ratios.

Finally, macroscopic and microscopic observation was made on the fractured surface of CT specimens for various Al6061-TiC composites and  $B/W$  ratios. Figs. 11 (a-c) show the fractograph of the fractured CT specimens surface with magnification of 1kX for various Al6061-TiC composites of  $a/W=B/W=0.5$ . From Fig.11 (a-c) the micromechanical failure mechanisms of composites show bimodal dimples and these dimples are characteristics of failure occurring by void nucleation, growth through the matrix and coalescence indicating ductile fracture. All the particles in the vicinity of crack tip are responsible for void nucleation by particle rupture and decohesion in the matrix. The crack initiation and fracture of the composites is mainly associated with voiding in the matrix around individual particles ahead of the main crack. Void initiation is more significant in the matrix near the interface. The micro-cracks grow from these micro-voids to absorb the energy. Crack propagates by linking these micro cracks locating the crack path preferentially in the matrix adjacent to the interface can be seen in Fig.12.

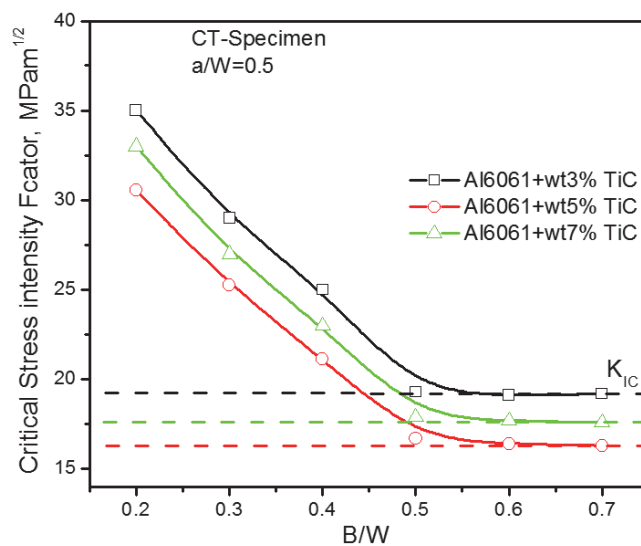


Figure 10: Variation of Critical stress intensity factor vs.  $B/W$  for various Al6061-TiC composites.

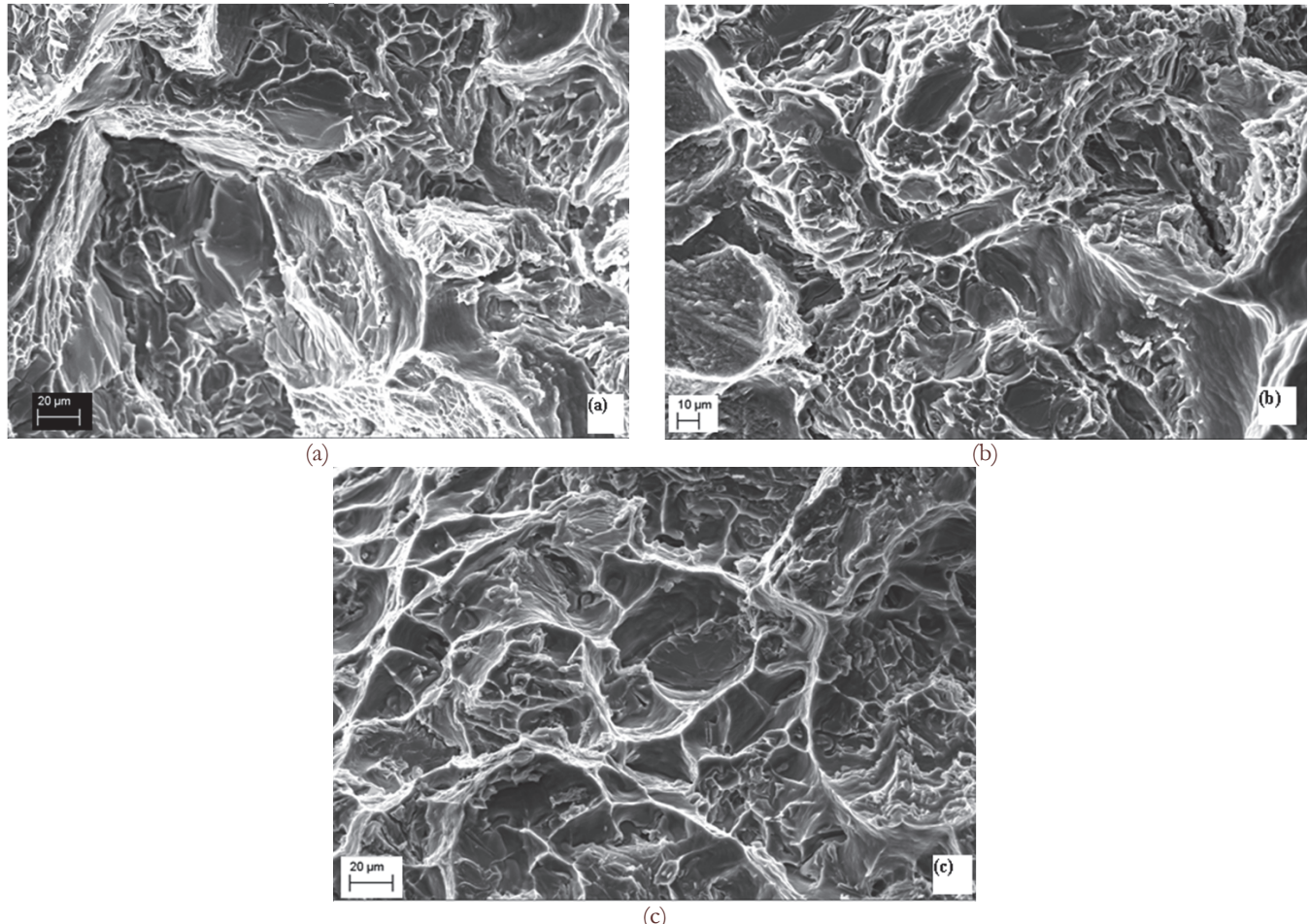


Figure 11: (a) SEM Fractographs of Al6061+3wt% TiC; (b) SEM Fractographs of Al6061+5wt % TiC; (c) SEM Fractographs of Al6061+7wt % TiC.

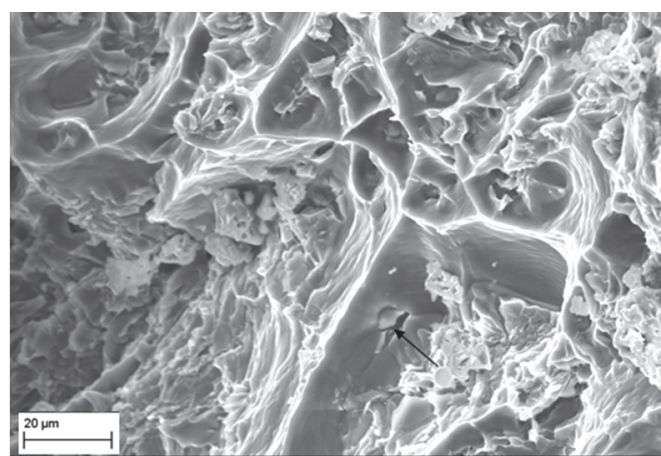


Figure 12: Matrix failure adjacent to Al/TiC interface for Al6061+5wt% TiC composite of  $a/W=B/W=0.5$ .

## CONCLUSIONS

Following are the major conclusions:

- (a) The fatigue crack growth rate curve for Al6061-TiC (3wt %-7wt %) metal matrix composites fall over a narrower stress intensity range. Hence, the composites may be considered for aerospace sectors.



(b) Void initiation is more significant in the matrix near the interface. The micro-cracks grow from these micro-voids to absorb the energy shows ductile fracture. Also, crack propagates by linking these micro cracks locating the crack path preferentially in the matrix adjacent to the interface.

(c) The variation of TiC reinforcement particles with Al6061 alloy matrix will affect the fracture toughness of the material. The fracture toughness of Al6061-TiC (3 wt %-7 wt %) metal matrix composites varied between 16.4 - 19.2 MPa $\sqrt{m}$  as compared to 25MPa $\sqrt{m}$  for base alloy Al6061 [18]. The solution treatment and age hardening process can further increase the toughness of these composites. The work can be extended to higher wt% TiC reinforcement particles with Al6061 alloy matrix. This remains as a future work.

## ACKNOWLEDGEMENTS

**T**he authors thank the Research centre, Bapuji Institute of Engineering & Technology, Davangere-577004, BiSS and TUV Rheinland, Bengaluru for their support in extending the testing facilities and helpful discussions.

## REFERENCES

- [1] McCartney, D.G., Grain refining of aluminium and its alloys using inoculants, *Int. Mater. Rev.*, 34 (1989) 247-260.
- [2] Mohanty, P.S., Gruzleski, J. E., Mechanism of grain refinement in aluminum, *Acta Metall. Mater.*, 43 (1995) 2001-2012.
- [3] Yang, Q., Senda, T., Ohmori, A., Effect of carbide grain size on microstructure and sliding wear behavior of HVOF-sprayed WC-12% Co coatings, *Wear*, 254 (2003) 23–34. DOI:10.1016/S0043-1648(02)00294-6.
- [4] Nukami, T., The growth of TiC particles in an Al matrix, *Materials Science Letters*, 17 (1998) 267-268.
- [5] Karantzalis, A.E., Lekatou, A., Georgatis, E., Poulas, V., Mavro, H., Microstructural Observations in a Cast Al-Si-Cu/TiC, Composite Materials Engineering and Performance, 10 (2009) 1-10.
- [6] Surappa, M.K., Rohatgi, P.K., Preparation and properties of aluminium alloy ceramic particle composites, *Journal of Material Science*, 16 (1981) 983-993.
- [7] Lloyd, D.J., Particle reinforced aluminum and magnesium matrix composites, *International Material Reviews*, 39 (1999) 1-23.
- [8] Fatchurrohman, N., Solidification characteristic of titanium carbide particulate reinforced aluminium alloy matrix composites, *Journal of Engineering Science and Technology*, 7 (2012) 248-256.
- [9] Raviraj, M.S., Sharanaaprabhu, C.M., Mohankumar, G.C., Experimental Analysis on Processing and Properties of Al-TiC Metal Matrix Composites, *Procedia Materials Science*, 5 (2014) 2032 – 2038.
- [10] Yu Qiao, Fracture toughness of composite materials reinforced by debondable particulates, *Scripta Materialia*, 49 (2003) 491–496. DOI:10.1016/S1359-6462(03)00367-1.
- [11] Rabiei, A., Vendra, L., Kishi,T., Fracture behavior of particle reinforced metal matrix composites, *Composites: Part A*, 39 (2008) 294–300.
- [12] Alaneme, K.K., Aluko, A.O., Fracture toughness ( $K_{IC}$ ) and tensile properties of as-cast and age-hardened aluminium (6063)-silicon carbide particulate composites, *Scientia Iranica, Transactions A: Civil Engineering* 19 (2012) 992–996.
- [13] Ajit Bhandakkar, Prasad, R.C., Sastry, M.L., Fracture Toughness of AA2024 Aluminum Fly Ash Metal Matrix Composites, *International Journal of Composite Materials*, 4(2) (2014) 108-124. DOI:10.5923/j.cmaterials.20140402.10.
- [14] ASTM E399-83, Standard test method for plane strain fracture toughness, Annual book of ASTM Standards, PA (2005).
- [15] Wilson, C., Landas, J. D., Fracture toughness testing with notched round bars, *ASTM-STP1360, Fatigue and Fracture Mechanics*, 30 (2000) 69-82.
- [16] Harrison, J.D., Fatigue Analysis of welded joints, *Metal Construction and British Welding Journal*, Mar. (1970) 93.
- [17] Mohanty, J.R., Verma, B.B., Ray, P.K., Evaluation of overload-induced fatigue crack growth retardation parameters using an exponential model, *Engineering Fracture Mechanics*, 75 (2008) 3941–3951.
- [18] Davidson, D.L., Tensile deformation and fracture toughness of 2014+15 vol. pct SiC particulated composite. *Metall. Trans*, 22A (1991) 113-123.